

Cresswell, A. J. , Sanderson, D. C.W. and Yamaguchi, K. (2018)
Assessment of the calibration of gamma spectrometry systems in forest
environments. *Journal of Environmental Radioactivity*, 181, pp. 70-77.
(doi: [10.1016/j.jenvrad.2017.10.019](https://doi.org/10.1016/j.jenvrad.2017.10.019))

This is the author's final accepted version.

There may be differences between this version and the published version.
You are advised to consult the publisher's version if you wish to cite from
it.

<http://eprints.gla.ac.uk/151046/>

Deposited on: 03 November 2017

Assessment of the calibration of gamma spectrometry systems in forest environments

Keywords Portable gamma spectrometry; Monte Carlo simulation; Forest environments

Abstract

A Monte Carlo simulation was used to develop a model of the response of a portable gamma spectrometry system in forest environments. This model was used to evaluate any corrections needed to measurements of ^{137}Cs activity per unit area calibrated assuming an open field geometry. These were shown to be less than 20% for most forest environments. The model was also used to assess the impact of activity in the canopy on ground level measurements. For similar activity per unit area in the lower parts of the canopy as on the ground, 10-25% of the ground based measurement would be due to activity in the canopy, depending on the depth profile in the soil. The model verifies that an optional collimator cap can assess activity in the canopy by repeat survey.

1. Introduction

Gamma spectrometry systems, either static in-situ or mobile measurements, are routinely used to determine radionuclide activity concentrations. Typically, these systems are calibrated assuming an open field geometry with laterally uniform activity concentrations and defined mass depths. However, in many situations these calibration assumptions will be invalid. Forest environments are one such example, of particular importance in Fukushima Prefecture where approximately

70% of the territory contaminated by the 2011 Fukushima Daiichi Nuclear Power Plant (FDNPP) accident is forested.

Forests present several different issues that should be considered. Differences in soil properties result in different rates of diffusion of activity down the soil column, and hence potentially different depth distributions from adjacent pasture or agricultural land. The trunks of trees shield the detector, which will reduce the count rate in a detector system compared to the same activity distribution on open ground. It is known that increasing source burial depth reduces the field of view of detectors in open ground (Tyler et.al. 1996), and thus it is expected that source depth will also be a variable in the effect of forestry on detected radiation. The canopy may contain activity that can potentially be measured by the detector system.

The work presented here uses Monte Carlo simulations of a typical portable gamma spectrometry backpack system, coupled with experimental verification. The system used for this work is based on a 76x76 mm cylindrical (3x3") NaI(Tl) detector, and is also equipped with an optional collimator cap to attenuate radiation from the canopy (Sanderson et.al. 2016). The expected implications for other detector systems are discussed.

Monte Carlo methods have been used to calculate dose rates from simulated activity distributions in open field and forested environments (Clovas et al., 1999; Malins et al., 2016). These methods have also been used to simulate the spectral response of NaI(Tl) detectors, at ground level and airborne survey heights, for open field geometries (Allyson, 1994; Allyson & Sanderson, 1998; Cresswell et al., 2001; Cresswell & Sanderson, 2012). The work presented here expands on these

earlier simulations, to simulate the spectral response of NaI(Tl) detectors to the more complex geometries presented by forest environments.

2. Methods

2.1 SUERC portable gamma spectrometer

The system used here comprises a 76x76 mm NaI(Tl) detector with digital spectrometer and integrated GPS receiver. This system has been used for the evaluation of remediation in forests in Fukushima Prefecture (Sanderson et al., 2016; Cresswell et al., 2016), and the calibration has been validated against known open field reference sites in the UK and Japan (Cresswell et al., 2013; Sanderson et al., 2013). A collimator, consisting of a plastic (nylon-6) 200 mm diameter and 150 mm height cylinder, with a 125 mm diameter and 100 mm depth central well, has been produced to attenuate radiation from above the detector. The system is shown schematically in Fig. 1. Angular response measurements in laboratory conditions using a ^{137}Cs (662 keV) source predict that this collimator attenuates 42% of radiation from above, and 22% of radiation from the ground in open field conditions (Sanderson et al., 2016; Buchanan et al., 2016).

2.2 Monte Carlo simulations

A Monte Carlo simulation of this detector system has been developed using GEANT4 (Agostinelli et al., 2003; Allison et al., 2006) (version 4.10.0 p-02, using the G4EMLOW 6.35 library). The model has been validated by reproducing the response of a naked 76x76 mm NaI(Tl) detector described in the literature (Heath, 1964), and the angular response

measurements for the backpack system with and without the collimator (Sanderson et al., 2016; Buchanan et al., 2016).

For the simulation of the Heath (1964) measurements a detector matching the description was used. For the backpack simulations the detector configuration matched the specifications of a Scionix Type 76 B 76 detector (<http://scionix.nl/standard2.htm>). The photomultiplier base unit including high voltage supply and digital spectrometer was matched to the Ortec digiBASE™ specification (<http://www.ortec-online.com/download/digiBASE.pdf>). These are detailed in the supplementary material, along with the external plastic canister, foam inserts, geographic positioning system (GPS) and collimator.

A simplified generic forest was modelled, shown schematically in Fig. 2. The physical properties of trees vary considerably between different species and environments. Pettersen (1984) lists the composition of dry wood from various species as consisting of 65-75% carbohydrates (cellulose and hemicellulose), 18-35% lignin and 4-10% of minor components. Nilklas & Spatz (2010) tabulate greenwood (50% water) densities for heartwood and sapwood, at 400-700 kg m⁻³ for most species, with conifers having lower densities. The model consists of trees with 50 cm diameter cylindrical trunks, composed of 35% cellulose, 15% lignin and 50% water (by mass) and a density of 400 kg m⁻³. The canopy is defined as a cubic volume on top of the trunks and extending half a tree spacing beyond the simulated forest, and consists of a uniform mixture of 50% air, 40% leaf and 10% wood (by volume), with the leaves a mixture of 50% water and 50% cellulose (by mass) with a density of 250 kg m⁻³. Two geometries were simulated, a low canopy with a base 2 m above the ground and a high canopy with a base 4 m above the ground. A

canopy base less than 2 m above the ground is common for Japanese cedar and many other species commonly found in Japanese forests. The simulation modelled 36 trees placed in a square pattern with spacings between the trunks variable, for the work presented here two different trunk spacings of 2 m and 3 m were used, corresponding to stand densities of approximately 2500 ha⁻¹ and 1000 ha⁻¹ respectively. The soil is of the composition described by Beck (1972); density 1600 kg m⁻³ with major elemental composition 26.2% Si, 5.9% Al, 2.6% Fe, 24.4% Ca, 0.9% H, 1.0% C, and 39.0% O. (oxide mass fractions: 67.5% SiO₂, 13.5% AlO₃, 10% H₂O, 4.5% Fe₂O₃, and 4.5% CO₂). It is recognised that the soil composition of forests, especially the litter and humic layers, will differ in composition and density from this. However, to first approximation, the mass attenuation coefficients for gamma radiation with energy >200 keV has been shown to be independent of composition (Cresswell & Sanderson, 2012). If activity profiles are expressed in terms of mass depth then the effect of density variation in the soil column is also accounted for. These materials are also described in more detail in the supplementary material.

Simulations were conducted for different source distributions. For activity on the ground, the simulations were conducted for uniformly distributed layers of zero thickness and 25 m radius at different linear depths, from which different depth distributions can be estimated by summing the outputs of each depth simulation. For activity in the canopy, the simulations were conducted for activity uniformly distributed in volumes of the canopy of thicknesses of 0.2 and 1.0 m. The counts in the full-energy peak in the simulated spectra were normalised to count rates per unit kBq m⁻² (for activity on the ground) or per Bq m⁻³ (for activity in the canopy). Simulations of activity in the soil were repeated with the trees removed to allow comparison with the open field

assumption of the calibration. Simulations were conducted with the detector in the centre of the simulated forest, at a height of 1.2 m and with a cuboid water operator (Buchanan et al., 2016). For all forest densities the detector was modelled in the centre of the forest (position A, Fig. 2). For the lower density forest, the operator was moved to two offset positions to evaluate the effect of changing geometry during a measurement, midway between trees in a row (position C, Fig. 2) and the midpoint between this and the centre point (position B, Fig. 2).

The geometry was restricted to allow a comparison between several different scenarios using a relatively small computing resource, and hence is finite. For open field conditions, activity at a mass depth of 1.0 g cm^{-2} , 90% of detected full energy radiation originates from within a radius of approximately 25 m in open field conditions (Tyler et.al. 1996). Thus, the limited geometry for activity on the ground (25 m radius) is not expected to be a significant effect. For activity in the canopy, the relatively small number of trees in the simulation restricts the area of the canopy, with solid angles less than 2π . Consideration of this geometrical effect will be needed in interpreting the simulation results, and the simulation data is used to aid in this interpretation.

2.3 Field validation

Field measurements are required to validate the results of the simulations. These were conducted in the forest adjacent to the former elementary school at Yamakiya, Kawamata town ($37^{\circ}36.169\text{N}$, $140^{\circ}40.582\text{E}$), approximately 40 km from the FDNPP. This site has been extensively investigated, with both backpack mapping (Cresswell et.al., 2016), soil sampling (Takahashi et al., 2015) and analysis of throughfall and litterfall (Hidasome et al., 2013; Kato & Onda, 2014; Kato et al., 2015). The site has a mainly deciduous forest to the east of the school

that has a gentle slope of approximately 5° from north to south, and a red pine stand to the north of the school which has a slightly steeper slope of approximately 10° from east to west, thus approximating to the level ground of the simulations. An observation tower has been constructed within the mainly deciduous area of the forest to allow direct measurements within the canopy. Both areas have a stand density of approximately 2500 ha^{-1} .

The protocol for the verification measurements was to repeat the area surveys conducted in 2014 and 2015 (Cresswell et al., 2016) to confirm that no substantial redistribution of activity has occurred, and to use this to select two locations for verification measurements, one within the mainly deciduous area where it is expected that the radiocaesium activity concentration in the canopy is low, and one within the red pine forest where it is anticipated that the radiocaesium activity concentration in the canopy is higher. Extended static measurements were conducted at these locations, both with and without the collimator fitted. The first location was used to verify the model for activity in the ground, and three soil cores were collected at this site in a triangular pattern with approximately 2 m spacing to estimate the ^{137}Cs activity per unit area and depth profile for this location. The second location was used to verify the model for activity in the canopy.

3. Results

3.1 Validation of detector response

Table 1 lists the efficiency and peak to total for mono-energetic sources at a distance of 10 cm from the detector face measured by Heath (1964) and simulated in this work, with a comparison

between the simulated spectrum for ^{137}Cs and the spectrum measured by Heath in Fig. 3. It can be seen that there is good agreement between the simulated and experimental responses.

Figure 4 shows a comparison between the simulated and measured angular response of the backpack system, using a ^{137}Cs source, with the 76x76 mm NaI(Tl) detector inside a plastic container that also includes a GPS receiver, photomultiplier tube, digital spectrometer and integrated HV supply, and plastic foam. The simulation slightly overestimates the full energy peak efficiency, especially for angles greater than 90° , but is overall in good agreement with the measurements. The measured spectra were not collected in a scatter free environment, and so include scattered energy components not present in the simulation. Figure 5 shows a corresponding comparison for the angular response of the detector with the collimator fitted.

The simulations slightly over estimate the detector efficiency compared to the measurements, especially for the downward angles ($>150^\circ$) passing through the photomultiplier and spectrometer which are not fully described in the model. The simulations including the collimator gave significantly greater efficiencies for the downward angles compared to the measured efficiencies. However, the simulated efficiencies for these angles were consistent with the simulated efficiencies without the collimator, as would be expected.

The simulations reproduce the properties of 76x76 mm NaI(Tl) detectors, both in isolation as described by Heath (1964) and within the SUERC portable gamma spectrometry system. Therefore, they are suitable for use in assessing the impact of forest environments on the calibration of such devices.

3.2 Simulations of detector fields of view

Simulations were conducted for activity on the surface of the ground, and on the underside of the high canopy, with a 3 m spacing between rows of trees, for a series of rings at increasing distance from the detector to 45 m. It is recognised that radiation from activity within the ground and canopy will be collimated, and hence these simulations represent the maximum field of view. Figure 6 shows the proportion of full energy peak signal within an increasing radius from the detector, for both activity on the ground and the canopy. The field of view for the low canopy would be similar to that for activity on the ground. These field of view simulations are similar to the earlier calculations (Tyler et al. 1996), with 90% of the full energy count rate originating within 25 m. Thus, the limited scale of the simulations conducted accounts for the majority of the radiation from an infinite source, and these simulations can be used to account for the effect of limited geometry in subsequent simulations. The extent of the simulated space for activity in the canopy is indicated by the dashed line in Fig. 6, indicating that for the activity in the canopy the simulations represent a minimum 60-70% of the field of view.

3.3 Simulation of attenuation by trees

Table 2 lists the peak count rates, normalised to 1 kBq m^{-2} activity per unit area, for simulations of an open field geometry and forests with spacings of 2 m and 3 m between the rows of trees. For the 3 m spacing two offset positions are also reported. It can be seen that the count rates recorded for the three different positions are identical within uncertainty. Therefore, these offset simulations were not repeated for the other tree spacing and the average response across the three positions was used.

206

207 The count rates for the forest simulations were lower than the count rates for the open field
208 simulations with the source at the same depth, as expected. The reductions relative to the open
209 field geometries are also given in Table 2. As would be expected, the attenuation of signal
210 originating from the ground is greater in the denser forests reflecting the increase in the average
211 mass between source and detector. Also, increasing the burial depth of the activity, which acts to
212 collimate the radiation reducing the contribution from radiation from greater distances that would
213 pass through a greater number of trees, reduces the influence of the forests.

214

215 3.4 Effect of activity in the canopy

216 The simulations for the 3 m spacing forest were repeated with the collimator in place to assess
217 the reduction in count rate this has on radiation from the ground. Simulations were also
218 conducted with activity uniformly distributed in the canopy, both with and without the
219 collimator. The count rates per unit activity concentration for these simulations are given in
220 Table 3.

221

222 It can be seen that for activity on the ground the collimator has a small effect, reducing the count
223 rate by less than 10%, with the effect reduced for greater source burial. This is less than the 22%
224 reduction calculated for the collimator effect from the measured angular response for open field
225 conditions. However, as noted the measured angular response includes significant attenuation for
226 radiation from below the detector which is unexpected, and not replicated in the simulated
227 response. In addition, the attenuation of radiation by the trees reduces the detector field of view,
228 and hence the influence of radiation from angles nearer 90° , in forests compared to open field

conditions. Since these angles are most affected by the collimator a reduced impact of the collimator in forests compared to open field conditions is expected.

For the activity in the canopy, simulations of activity in 20 cm thick slices of the canopy (Table 3) show that activity more than 1 m above the base of the canopy is attenuated by the canopy to the extent that this does not contribute to the detector response. Simulations have therefore been conducted for measurements with and without the collimator, for activity uniformly distributed in the lower 1 m of the canopy, for a canopy with a base at 2 m above the ground (the ‘low canopy’) and a canopy with a base at 4 m above the ground (the ‘high canopy’), for trees with 3 m spacing. The results of these simulations are also summarised in Table 3. It can be seen that for the higher canopy the count rate is slightly reduced, reflecting the reduced solid angle for the source. Using the difference in the proportion of signal from within the area simulated in Fig. 6, the simulated 0.22 ± 0.02 cps would correspond to 0.25 ± 0.02 cps accounting for the geometric effect, consistent with the count rate for the low canopy. The overall effect of the collimator is similar for both canopy base heights, with a slightly reduced effect for the high canopy.

In reality, it is unlikely that the canopy density and composition, nor the activity distribution within the canopy, would be uniform, and canopy heights would be variable. Thus, variations on the model may be needed to fit the outcomes to particular parameters of each forest.

3.4 Verification of model through field measurements

Measurements were taken in the forest by the former Yamakiya elementary school in May 2016, with soil cores collected. Following a resurvey of the forest to confirm no significant

redistribution of activity had occurred since the previous surveys in 2015 (Cresswell et al., 2016), two locations were selected for static measurements with and without the collimator. The first was a level section of forest with almost entirely Japanese oak of a similar age (trunk diameters between 30 and 40 cm) and a gradient in the radiocaesium activity per unit area of about 10% over a distance of 20-30 m. Previous measurements of samples from deciduous trees (Kato & Onda 2014, Kato et al. 2015) indicate that the activity in the canopy of these deciduous trees would be very small. This site was selected to evaluate the attenuation of radiation on the ground, and three soil cores were taken at a distance of approximately 2 m from the measurement point to allow an estimation of the radiocaesium activity distribution from which the expected open field response of the detector could be determined. It is recognised that small scale heterogeneity is expected, and that three cores are inadequate to fully characterise the site. For the establishment of calibration sites, practice established in the UK and Europe (Sanderson et al., 2013; Tyler et al., 1996; Sanderson et al., 2003, 2004) is to collect a much larger number of cores in a spatially representative manner. However, when resource is limited a smaller number have been used previously to produce a reasonable estimate of the activity per unit area on a site (Sanderson et al., 2003, 2004). The second site was a small stand of Red Pine, where it was hoped that the activity in the canopy would be more significant. This site was slightly sloping, with a slightly larger gradient in radiocaesium activity per unit area. The pine trees were tall, more than 10 m, and covered a small area of 20-30 m dimensions, with some Japanese oak and other deciduous trees mixed in. It is recognised that the combination of the small stand size and high canopy, with intervening deciduous canopy, results in less than ideal conditions with a reduced solid angle for activity in the canopy and intervening attenuating material. This site was

specifically selected to evaluate the collimator effect, and no soil samples were collected. Fuller details of the samples and measurements are given in the Supplementary Material.

The results of the measurements are summarised in Table 4. For the effect of the attenuation by the trees these are constrained by the relatively large dispersion in the soil core data, resulting in a large uncertainty in the ^{137}Cs activity per unit area and associated expected open field count rate.. The reduction in ^{137}Cs count rate compared to the open field calibration was, however, consistent with the output from the model (measured $12 \pm 9\%$, modelled $15 \pm 5\%$). For the measurements of the effect of the collimator, measurements in both the areas dominated by oak and with the pine stand were consistent with the simulations with no measurable activity in the canopy (measured $8 \pm 8\%$ and $-1 \pm 10\%$, modelled $8 \pm 3\%$). It is likely that the measurements in the pine stand were influenced by the small solid angle of the pine stand with the very high canopy, and attenuation by intervening deciduous canopy, and potentially by a low concentration of activity retained in the canopy. It will be necessary to locate a forest area that covers a larger area, with a low canopy and known to retain significant activity in the canopy to verify the modelled response of the detector with the collimator fitted to activity in the canopy.

4. Discussion and Conclusions

A Monte Carlo code was developed using GEANT4 to model the response of backpack systems in forest environments. This code was validated by simulation of a 76x76 mm NaI(Tl) matching that described by Heath (1964), with excellent agreement between the simulation conducted in this work with these measurements. The detector system was then modified to match the 76x76 mm NaI(Tl) detector in the SUERC portable gamma spectrometry system, with the associated

container and electronics. Simulations of point ^{137}Cs sources in a large open volume were conducted with the source at different azimuthal angles around the detector. These were compared with laboratory measurements conducted on a bench top, and hence presenting a large scattered energy component in the spectra. Again, these show good agreement between simulation and measurement, although the efficiencies calculated from the simulation are slightly higher than the measurements.

The SUERC portable gamma spectrometry system also includes an optional collimator cap, designed to attenuate radiation from above the detector by approximately 50%. This was also included in the model, and compared with a corresponding set of laboratory measurements. In this case, the agreement between experimental measurements and simulation was not as good. The simulation predicted a significantly larger efficiency, and a smaller reduction in efficiency with the cap fitted, than the measurements. This is particularly evident for geometries with the source below the detector. For these geometries the collimator introduces less additional shielding, which is reflected in the simulation with the experimental data showing a reduction in efficiency with the collimator at these positions, hence there is likely to be an additional factor in the experiment that has not been accounted for. However, it is noted that this effect is not significant for activity in the canopy where the radiation source is above the detector where the simulation and measurements are in better agreement.

These simulations of point sources indicate that the model satisfactorily reproduces experimental measurements of the SUERC portable gamma spectrometry system, and therefore is suitable for evaluating the response of this system in forest environments. A model was developed of a

simplified, generic forest, and used to simulate the response of the backpack system to activity in the soil and the canopy, both with and without the collimator. Measurements collected from a forest area in Fukushima were consistent with the outputs from the model.

For activity on the ground, the primary question is the extent to which attenuation by trees affects the measured activity per unit area for systems calibrated assuming an open field geometry. The simulations have shown a maximum effect for activity on the surface, with the reduction in count rate as a result of attenuation by the trees decreasing with increasing depth of activity. This is consistent with a combination of the detector field of view being reduced with increased source depth, and hence reduced influence of gamma rays from more distant locations that pass through a larger biomass, and the reduction in the proportion of the total mass depth radiation passes through from the trees. As expected, the effect is also larger for increased density of the forest. The position of the detector relative to the trees in these simulations had little or no effect on the simulated count rate.

The maximum effect for these simulations has been for a dense forest with a stand density of approximately 2500 ha⁻¹ of large trees with 50 cm diameter trunks, where for surface activity the backpack would underestimate the activity per unit area by 35% if calibrated to open field conditions. The majority of forests would have either lower stand densities, or smaller trees, and activity that is not on the surface, and the underestimation of activity per unit area would therefore be less than this. The simulations conducted suggest that corrections of less than 20% would need to be applied in all but a few cases, and that in many cases corrections of less than 10% would be needed.

The simulations of activity in the canopy showed that, for the canopy density used here, gamma rays from ^{137}Cs do not significantly penetrate more than 1 m in the canopy. The geometry of the simulation models a source-detector solid angle which is less than 2π , and some geometrical corrections to account for the change in solid angle when the base of the canopy is increased need to be applied. After these corrections, the count rate per unit activity in the canopy was independent of the height of the canopy base. It is noted that the simulated count rate for the same activity distributed in the canopy was significantly less than on the ground, by approximately a factor of four if the activity in the canopy was distributed in a 1 m depth, with the exact comparison dependent on the activity distribution in the soil and canopy. Therefore, the influence of activity in the canopy on the measured activity per unit area was small unless the activity in the canopy was greater than that on the ground.

With the collimator fitted, the simulations predict a reduction in count rate from activity in the canopy of $43 \pm 5\%$, and less than 10% from activity on the ground. This is very similar to the count rate reduction from above calculated from the measurements of angular response (42%), although these measurements predicted a larger reduction in count rate for activity on the ground (22%) which in part would be explained by the reduction in efficiency measured below the detector despite no additional shielding present.

The simulation of the collimated system demonstrates that a two-step survey, with and without the collimator, would allow an estimation of activity within the canopy. For the simplified forest simulated here, with activity distributed uniformly throughout the canopy, a reduction in count

366 rate of 1 cps by using the collimator would correspond to a ^{137}Cs activity per unit volume in the
367 canopy of $9.1 \pm 1.8 \text{ kBq m}^{-3}$, corresponding to $36 \pm 7 \text{ Bq kg}^{-1}$.

368

369 The model presented here has been developed specifically for the SUERC portable gamma
370 spectrometry system operated as a backpack detector, however the results are applicable to other
371 systems within forests and the method may be readily extended to other environments.

372

373

Associated content

Table S.1: Description of different compartments within the model.

Figure S.1: ^{137}Cs distribution around the former Yamakiya Elementary School, showing areas of Japanese oak (northern circle) and red pine stands (southern circle) identified for measurements to validate the forest model.

Figure S.2: Location of measurement point (red star) and soil sampling locations (red dots) in the area of the forest by the former Yamakiya elementary school dominated by Japanese oak. The black circles indicate the location of the trees closest to the measurement point.

Table S.2: Laboratory gamma spectrometry results on three cores collected from the forest site near the former Yamakiya elementary school.

Table S.3: Activity per unit area and mass depth for each core collected from the forest site near the former Yamakiya elementary school.

Acknowledgments

Validation measurements were conducted at the Yamakiya Elementary School grounds and the surrounding forest with the permission of Kawamata Town Office and the assistance of Hiroaki Kato (Center for Research in Isotopes and Environmental Dynamics, University of Tsukuba, 1-1-1 Tennodai, Tsukuba, Ibaraki 305-8572, Japan), Kiri Asano and Atsuko Chiba (Institute of Environmental Radioactivity). Laboratory gamma spectrometry was conducted at the Institute of Environmental Radioactivity with the assistance of Tsugiko Takase

References

- S. Agostinelli , Allison, J., Amako, K., Apostolakis, J., Araujo, H., Arce, P., Asai, M., Axen, D.,
Banerjee, S., Barrant, G., Behner, F., Bellagamba, L., Boudreau, J., Broglia, L., Brunengo,
A., Burkhardt, H., Chauvie, S., Chuma, J., Chytrcek, R., Cooperman, G., Cosmo, G.,
Degtyarenko, P., Dell'Acqua, A., Depaola, G., Dietrich, D., Enami, R., Feliciello, A.,
Ferguson, C., Fesefeldt, H., Folger, G., Foppiano, F., Forti, A., Garelli, S., Giani, S.,
Giannitrapani, R., Gibin, D., Gomez Cadenas, J.J., Gonzalez, I., Gracia Abril, G., Greeniaus,
L.G., Greiner, W., Grichine, V., Grossheim, A., Gumplinger, P., Hamatsu, R., Hashimoto, K.,
Hasui, H., Heikkinen, A., Howard, A., Ivanchenko, V., Johnson, A., Jones, F.W., Kallenbach,
J., Kanaya, N., Kawabata, M., Kawabata, Y., Kawaguti, M., Kelner, S., Kent, P., Kodama, T.,
Kokoulin, R., Kossov, M., Kurashige, H., Lamanna, E., Lampen, T., Lara, V., Lefebure, V.,
Lei, F., Liendl, M., Lockman, W., Longo, F., Magni, S., Maire, M., Medernach, E.,
Minamimoto, K., Mora de Freitas, P., Morita, Y., Murakami, K., Nagamatu, M., Nartallo, R.,
Nieminen, P., Nishimura, T., Ohtsubo, K., Okamura, M., O'Neale, S., Oohata, Y., Paech, K.,
Perl, J., Pfeiffer, A., Pia, M.G., Ranjard, F., Rybin, A., Sadilov, S., Elvio Di Salvo, Santin, G.,
Sasaki, T., Savvas, N., Sawada, Y., Scherer, S., Sei, S., Sirotenko, V., Smith, D., Starkov, N.,
Stoecker, H., Sulkimo, J., Takahata, M., Tanaka, S., Tcherniaev, E., Safai, F. Tehrani, M.
Tropeano, Truscott, P., Uno, H., Urban, L., Urban, P., Verderi, M., Walkden, A., Wander, W.,
Weber, H., Wellisch, J.P., Wenaus, T., Williams, D.C., Wright, D., Yamada, T., Yoshida, H.,
Zschesche, D. 2003. Geant4—a simulation toolkit. Nuclear Instruments and Methods in
Physics Research A 506, 250-303; doi:10.1016/S0168-9002(03)01368-8

Allison, J.; Amako, K.; Apostolakis, J.; Araujo, H.; Arce Dubois, P.; Asai, M.; Barrand, G.;
 Capra, R.; Chauvie, S.; Chytrcek, R.; Cirrone, G. A. P.; Cooperman, G.; Cosmo, G.; Cuttone,
 G.; Daquino, G. G.; Donszelmann, M.; Dressel, M.; Folger, G.; Foppiano, F.; Generowicz, J.;
 Grichine, V.; Guatelli, S.; Gumplinger, P.; Heikkinen, A.; Hrivnacova, I.; Howard, A.; Incerti,
 S.; Ivanchenko, V.; Johnson, T.; Jones, F.; Koi, T.; Kokoulin, R.; Kossov, M.; Kurashige, H.;
 Lara, V.; Larsson, S.; Lei, F.; Link, O.; Longo, F.; Maire, M.; Mantero, A.; Mascialino, B.;
 McLaren, I.; Mendez Lorenzo, P.; Minamimoto, K.; Murakami, K.; Nieminen, P.; Pandola,
 L.; Parlati, S.; Peralta, L.; Perl, J.; Pfeiffer, A.; Pia, M. G.; Ribon, A.; Rodrigues, P.; Russo,
 G.; Sadilov, S.; Santin, G.; Sasaki, T.; Smith, D.; Starkov, N.; Tanaka, S.; Tcherniaev, E.;
 Tome, B.; Trindade, A.; Truscott, P.; Urban, L.; Verderi, M.; Walkden, A.; Wellisch, J. P.;
 Williams, D. C.; Wright, D.; Yoshida, H., 2006. Geant4 developments and applications. IEEE
 Transactions on Nuclear Science 53, 270-278; doi 10.1109/TNS.2006.869826
 Allyson, J.D., Sanderson, D.C.W., 1998. Monte Carlo simulation of environmental airborne
 gamma-spectrometry. J. Environ. Radioact. 38, 259–282.
 Allyson, J.D., 1994. Environmental gamma ray spectrometry: simulation of absolute calibration
 of in-situ and airborne spectrometry for natural and anthropogenic sources. PhD Thesis,
 University of Glasgow.
 Beck, H.L, Decampo J., Gogolak, C., 1972. In-situ Ge(Li) and NaI(Tl) gamma-ray spectrometry.
 Health and Safety Laboratory, United States Atomic Energy Commission, report HASL-258,
<http://www.osti.gov/scitech/servlets/purl/4599415/>
 Buchanan, E., Cresswell, A.J., Seitz, B., Sanderson, D.C.W, 2016. Operator related attenuation
 effects in radiometric surveys. Radiation Measurements 86, 24-31; doi
 10.1016/j.radmeas.2015.15.029.

440 Clouvas, A., Xanthos, S., Antonopoulos-Domis, M., Alifragis, D. A., 1999. Contribution of Cs-
 441 137 to the total absorbed gamma dose rate in air in a Greek forest ecosystem: Measurements
 442 and Monte Carlo computations. *Health Physics* 76, 36-43.

443 Cresswell, A.J., Kato, H., Onda, Y., Nanba, K., 2016. Evaluation of Forest Decontamination
 444 Using Radiometric Measurements. *J. Environ. Radioact.*, doi:10.1016/j.jenvrad.2016.07.024

445 Cresswell, A.J., Sanderson, D.C.W., Harrold, M., Kirley, B., Mitchell, C., Weir, A., 2013.
 446 Demonstration of lightweight gamma spectrometry systems in urban environments *J. Environ.*
 447 *Radioact.* 124, 22-28; doi: 10.1016/j.jenvrad.2013.03.006

448 Cresswell, A.J., Sanderson, D.C.W., 2012. Evaluating airborne and ground based gamma
 449 spectrometry methods for detecting particulate radioactivity in the environment: A case study
 450 of Irish Sea beaches. *Science of the Total Environment* 437, 285–296.

451 Cresswell, A.J., Allyson, J.D., Sanderson, D.C.W., 2001. A code to simulate nuclear reactor
 452 inventories and associated gamma-ray spectra. *J. Environ. Radioact.* 53, 399–410.

453 Heath, R.L., 1964. Scintillation Spectrometry: Gamma-ray Spectrum Catalogue. Gamma-ray
 454 Spectrometry Center, Idaho National Engineering & Environmental Laboratory, report IDO-
 455 16880-1. Revised Electronic Update 1997,
 456 http://sites.fas.harvard.edu/~phys191r/Bench_Notes/B1/NAI_catalog.pdf

457 Hisadome, K., et al., 2013. Migration of radiocaesium with litterfall in hardwood-Japanese red
 458 pine mixed forest and sugi plantation. *Journal of the Japanese Forest Society* 95(5), 267-274.

459 Kato, H., Onda, Y., Hisadome, K., Loffredo, N., Kawamori, A., 2015. Temporal changes in
 460 radiocesium deposition in various forest stands following the Fukushima Dai-ichi Nuclear
 461 Power Plant accident. *J. Environ. Radioact.* doi:10.1016/j.jenvrad.2015.04.016

462 Kato, H., Onda, Y., 2014. Temporal changes in the transfer of accidentally released ^{137}Cs from
 463 tree crowns to the forest floor after the Fukushima Daiichi Nuclear Power Plant accident.
 464 Progress in Nuclear Science and Technology 4, 18-22.

465 Malins, A., Kurikami, H., Nakama, S., Saito, T., Okumura, M., Machida, M., Kitamura, A.,
 466 2016. Evaluation of ambient dose equivalent rates influenced by vertical and horizontal
 467 distribution of radioactive cesium in soil in Fukushima Prefecture. J. Environ. Radioact. 151,
 468 38-49.

469 Niklas, K.J., Spatz, H-C., 2010. Worldwide correlations of mechanical properties and green wood
 470 density. American Journal of Botany 97, 1587-1594.

471 Pettersen, R.C. 1984. The Chemical Composition of Wood. In: Rowell R.M. (ed) The Chemistry
 472 of Solid Wood, Advances in Chemistry series, 207, chapter 2, DOI: 10.1021/ba-1984-
 473 0207.ch002

474 Sanderson, D.C.W., Cresswell, A.J., Tamura, K., Iwasaka, T., Matsuzaki, K., 2016. Evaluating
 475 remediation of radionuclide contaminated forest near Iwaki, Japan, using radiometric
 476 methods. J. Environ. Radioact. 162-163, 118-128; doi: 10.1016/j.jenvrad.2016.05.019.

477 Sanderson, D.C.W., Cresswell, A.J., Seitz, B.; Yamaguchi, K., Takase, T., Kawatsu, K., Suzuki,
 478 C., Sasaki, M., 2013. Validated Radiometric Mapping in 2012 of Areas in Japan Affected by
 479 the Fukushima-Daiichi Nuclear Accident. Glasgow:University of Glasgow, 2013. ISBN 978-
 480 0-85261-937-7. <http://eprints.gla.ac.uk/86365/>

481 Sanderson D.C.W., Cresswell A.J., Scott E.M., Lang J.J., 2004. Demonstrating the European
 482 Capability for Airborne Gamma Spectrometry: results from the ECCOMAGS Exercise.
 483 Radiation Protection Dosimetry 109, 119-125.

484 Sanderson, D.C.W., Cresswell, A.J., Lang, J.J. (Eds.), 2003. An International Comparison of
485 Airborne and Ground Based Gamma Ray Spectrometry. Results of the ECCOMAGS 2002
486 Exercise held 24th May to 4th June 2002, Dumfries and Galloway, Scotland. Glasgow:
487 University of Glasgow, ISBN 0 85261 783 6.

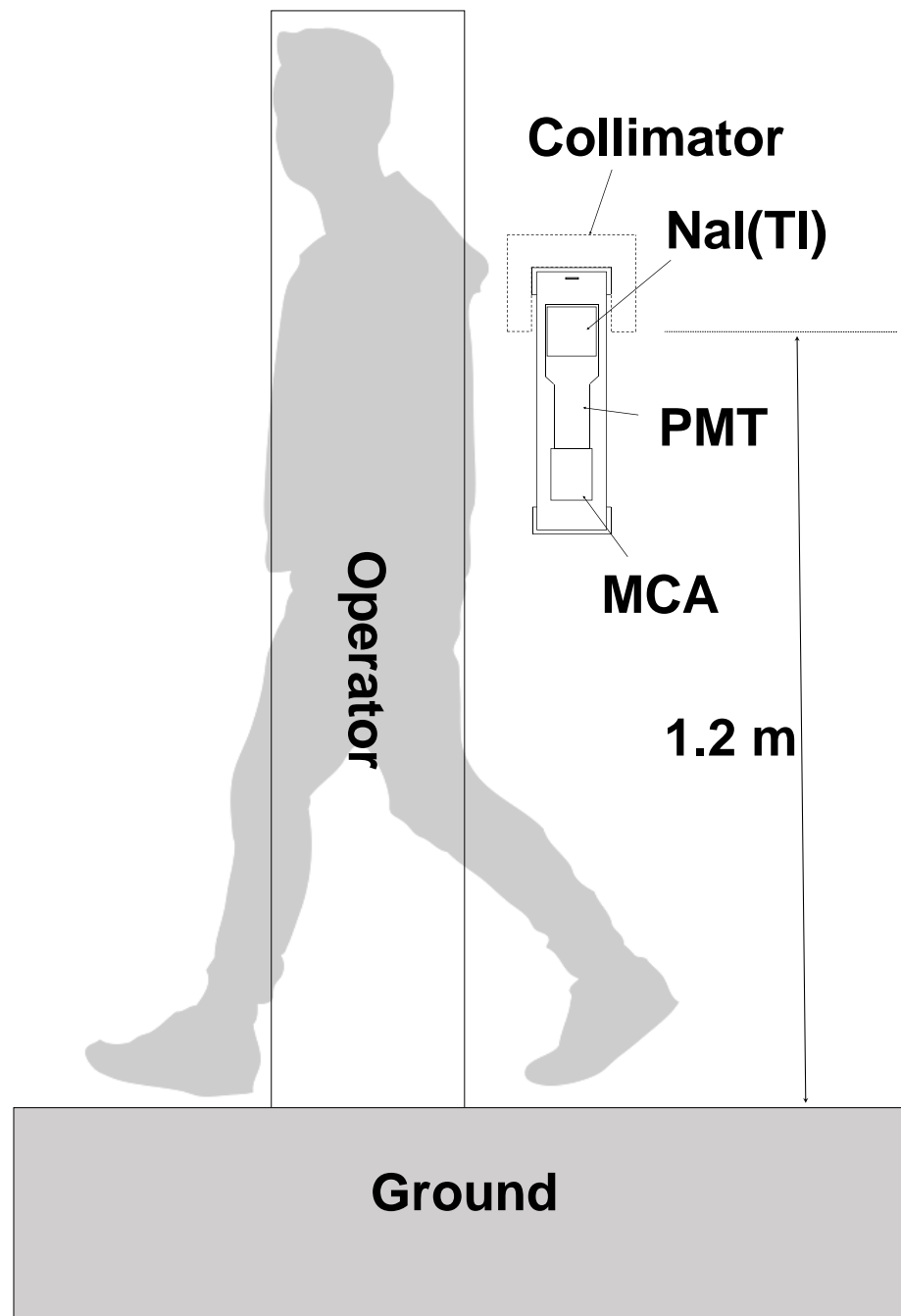
488 Takahashi, J., Tamura, K., Suda, T., Matsumura, R., Onda, Y., 2015. Vertical distribution and
489 temporal changes of ^{137}Cs in soil profiles under various land uses after the Fukushima Dai-
490 ichi Nuclear Power Plant accident. J. Environ. Radioact. 139, 351-361, DOI
491 10.1016/j.jenvrad.2014.07.004

492 Tyler, A.N., Sanderson, D.C.W., Scott, E.M., Allyson, J.D., 1996. Accounting for spatial
493 variability and fields of view in environmental gamma ray spectrometry. J. Environ. Radioact.
494 33, 213-235.

495

496

497



498 **Figure 1.** Schematic of the backpack system consisting of a NaI(Tl) crystal with photomultiplier
 499 (PMT) and digital multi-channel analyser (MCA) in a weather proof canister, and optional
 500 collimator (dashed line). The centre of the crystal is at a height of approximately 1.2 m. For the
 501 simulation, a cuboid shaped operator is used (Buchanan et al., 2016).

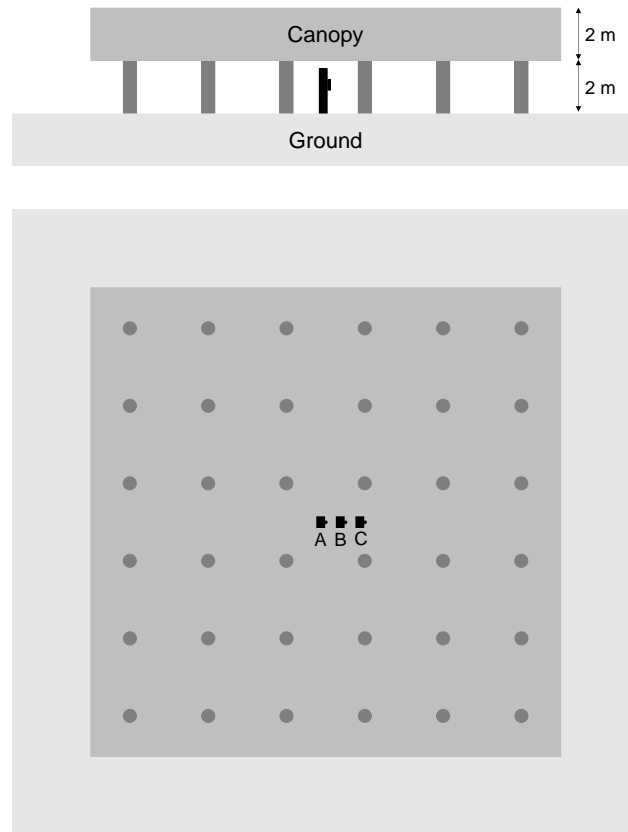


Figure 2. Schematic of simplified forest geometry, with a low canopy, showing three detector positions (A, B and C) used. Simulations with a high canopy (base 4 m above ground and 10 m height) have also been conducted.

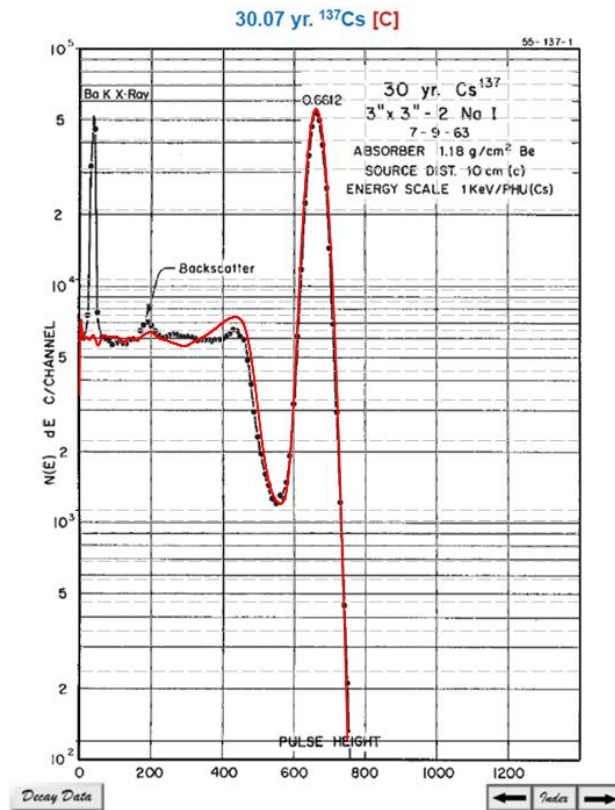


Figure 3. Comparison between the simulated spectrum (red) for a ^{137}Cs source at 10 cm from a $3\times 3''$ NaI(Tl) detector, and the spectrum measured by Heath (1964). Note that the simulation does not include the Ba x-ray.

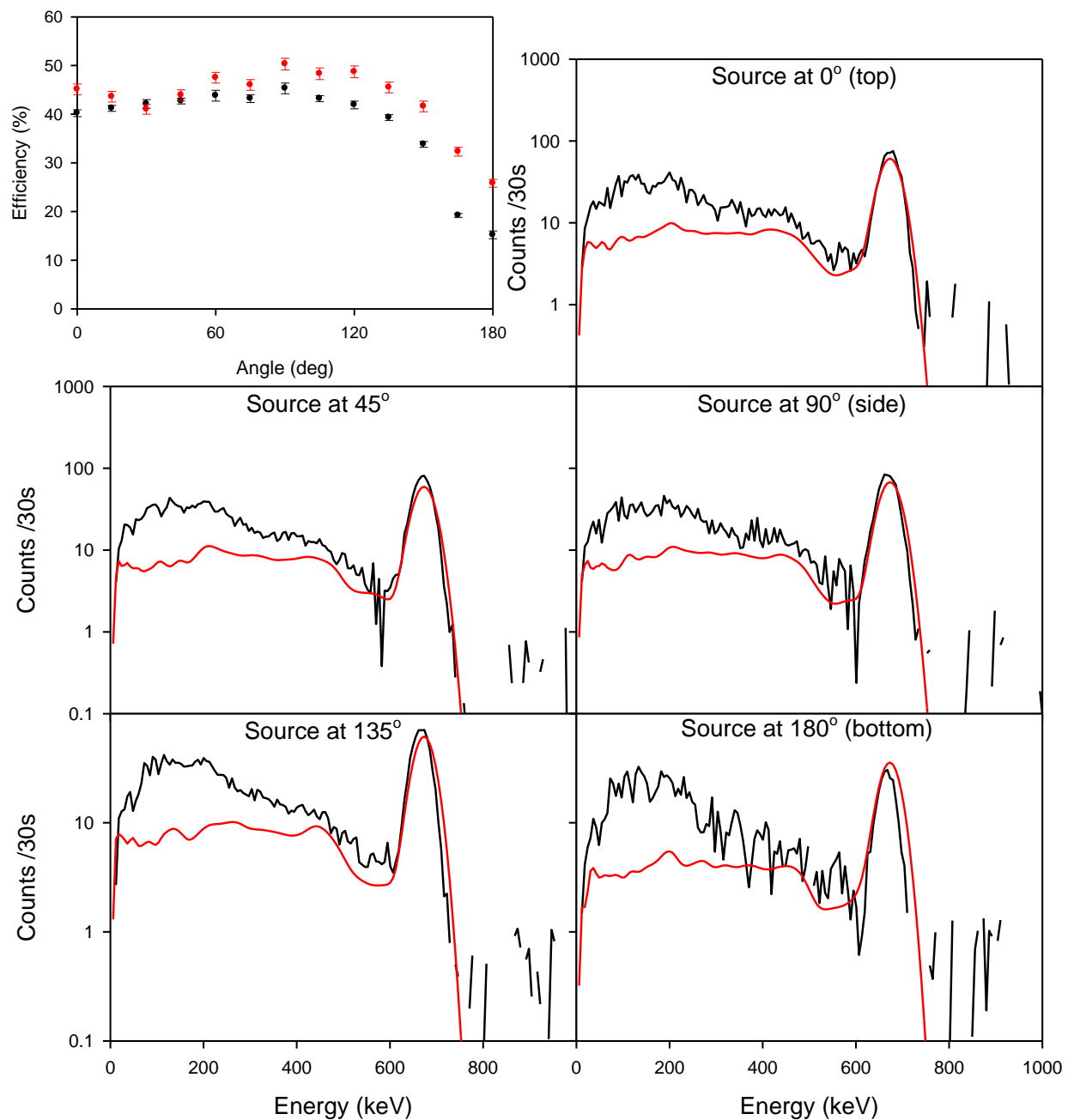


Figure 4. Comparison between simulated (red) and measured (black) angular response for the backpack system (top left) with spectra at selected angles.

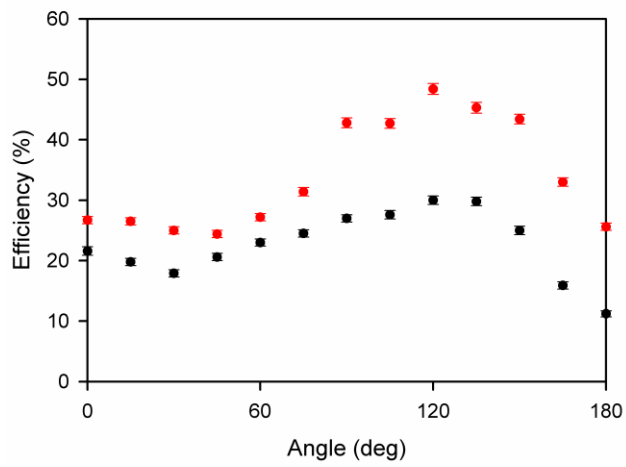


Figure 5. Comparison between simulated (red) and measured (black) angular response for the backpack system with the collimator fitted.

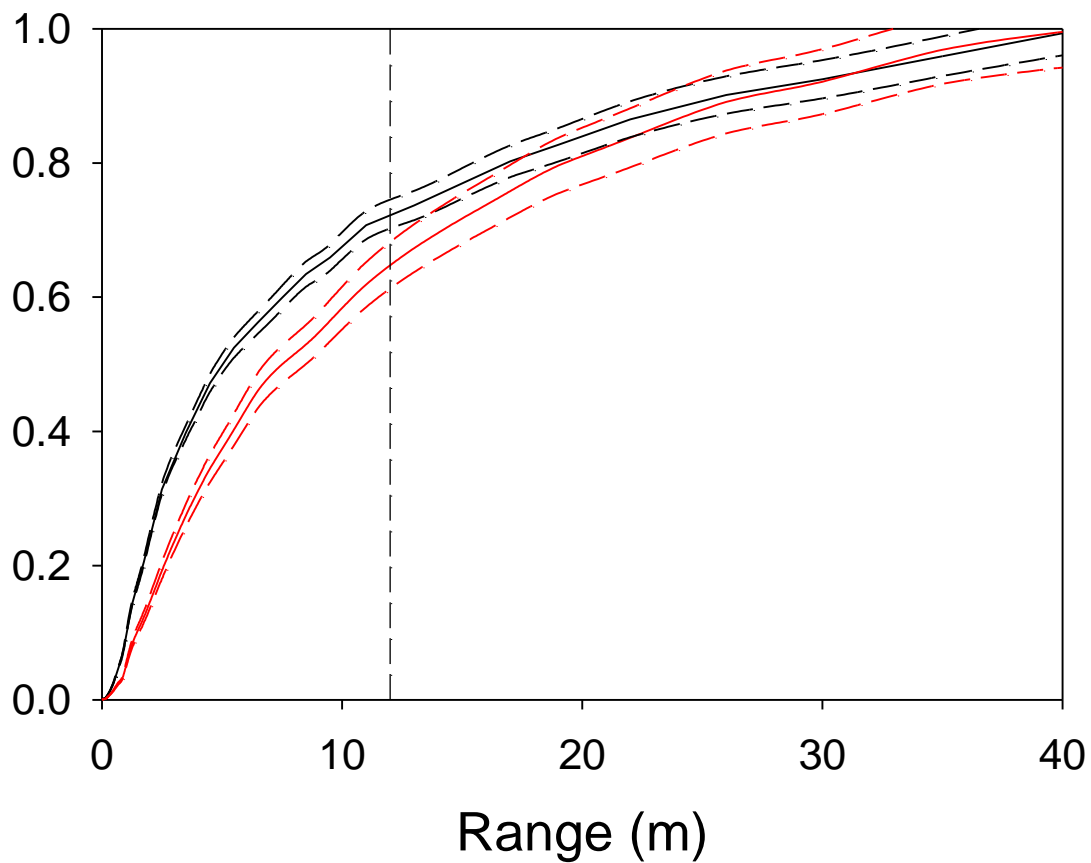


Figure 6. Proportion of simulated ^{137}Cs full energy count rate as a function of range for activity on the ground surface (black) and the underside of the high canopy (red).

524 **Table 1.** Comparison between total efficiency and peak to total values measured by Heath
525 (1964) and simulated in this work for three mono-energetic gamma emitting radionuclides at 10
526 cm distance from the detector face.

	Total Efficiency		Peak to Total	
	Measured	Simulated	Measured	Simulated
¹³⁷ Cs	0.0202	0.0195 ± 0.0001	0.536	0.528 ± 0.006
⁴⁷ Sc	0.0303	0.0283 ± 0.0002	0.960	0.900 ± 0.008
⁸⁸ Y	0.0150	0.0146 ± 0.0003	0.280	0.287 ± 0.002

527

Table 2. Simulated count rates per unit activity per unit area, for different tree spacing, offsets and source depths, with reductions relative to open field conditions.

Depth (g cm ⁻²)	Position	Open field (cps (kBq m ⁻²) ⁻¹)	3 m spacing (cps (kBq m ⁻²) ⁻¹)	Reduction (%)	2 m spacing (cps (kBq m ⁻²) ⁻¹)	Reduction (%)
0	A	2.05 ± 0.08	1.68 ± 0.05	18.0 ± 4.4	1.34 ± 0.05	34.6 ± 4.5
	B		1.64 ± 0.05	19.9 ± 4.5		
	C		1.69 ± 0.05	17.6 ± 4.4		
	average		1.67 ± 0.03	18.5 ± 4.0		
0.8	A	1.36 ± 0.07	1.17 ± 0.06	14.4 ± 6.6	0.98 ± 0.04	28.3 ± 5.7
	B		1.16 ± 0.04	14.6 ± 5.8		
	C		1.12 ± 0.04	17.9 ± 5.8		
	average		1.15 ± 0.03	15.6 ± 5.3		
1.6	A	1.00 ± 0.04	0.87 ± 0.04	13.1 ± 6.1	0.82 ± 0.04	17.6 ± 6.0
	B		0.94 ± 0.04	6.1 ± 5.7		
	C		0.92 ± 0.05	8.1 ± 6.4		
	average		0.91 ± 0.02	9.1 ± 4.9		
2.4	A	0.79 ± 0.04	0.72 ± 0.05	8.2 ± 7.8	0.61 ± 0.03	22.0 ± 6.4
	B		0.70 ± 0.03	10.6 ± 6.4		
	C		0.78 ± 0.03	1.3 ± 6.6		
	average		0.73 ± 0.02	6.7 ± 5.7		

Table 3. Simulated count rates per unit activity per unit area for activity on the ground, and per unit activity per unit volume for activity in the canopy (low canopy with a base 2 m above ground, high canopy with a base 4 m above ground), with and without the collimator.

Geometry	Without collimator (cps (kBq m ⁻²) ⁻¹)	With collimator (cps (kBq m ⁻²) ⁻¹)	Reduction (%)
On ground, 0 g cm ⁻² depth	1.67 ± 0.03	1.51 ± 0.11	9.6 ± 6.6
In ground, 1.6 g cm ⁻² depth	0.91 ± 0.02 (cps (kBq m ⁻³) ⁻¹)	0.97 ± 0.09 (cps (kBq m ⁻³) ⁻¹)	-6.6 ± 9.9
In low canopy, 2.0-2.2 m above ground	0.65 ± 0.05		
In low canopy, 2.2-2.4 m above ground	0.20 ± 0.03		
In low canopy, 2.4-2.6 m above ground	0.15 ± 0.03		
In low canopy, 2.6-2.8 m above ground	0.05 ± 0.02		
In low canopy, 2-3 m above ground	0.26 ± 0.02	0.15 ± 0.01	43 ± 5
In high canopy, 4-5 m above ground	0.22 ± 0.02	0.15 ± 0.01	31 ± 4

Table 4. Summary of measurements conducted at Yamakiya school forest, showing the activity per unit area and relaxation mass depth determined from soil samples, with the expected count rate for open field condition, and the measured count rates with and without the collimator cap. The reduction compared to open field conditions corresponds to attenuation by the trees, and for the collimated measurements compared to uncollimated the effect of the collimator.

Site	¹³⁷ Cs		Open field	Uncollimated	Reduction relative to open field	Collimated	Reduction relative to uncollimated
	kBq m ⁻²	g cm ⁻²	cps	cps	(%)	cps	(%)
Oak	365 ± 268	0.85 ± 0.33	610 ± 450	540 ± 30	12 ± 9	497 ± 30	8.0 ± 8.2
Pine				589 ± 48		598 ± 29	-1.5 ± 9.3